

研究成果の刊行に関する一覧表

書籍

著者名	論文タイトル	書籍全体の編集者名	書籍名	出版社名	出版地	出版年	ページ
橋口昭大、高嶋 博	Charcot-Marie-Tooth病の網羅的遺伝子診断	鈴木則宏、祖父江元、荒木信夫、宇川義一、川原信隆	Annual Review 神経 2012	中外医学社	東京	2012	267-273
中川正法	Charcot-Marie-Tooth病に対する治療の進歩	鈴木則宏、祖父江元、荒木信夫、宇川義一、川原信隆	Annual Review 神経 2013	中外医学社	東京	2013	211-222
山野嘉久	HAM (HTLV-1 関連脊髄症)	大生定義	すべての内科医が知っておきたい神経疾患の診かた、考え方とその対応	羊土社	東京	2012	279-281

雑誌

著者名	論文題名	発表誌名	巻号	ページ	出版年
Yuan J, Matsuura E, Higuchi Y, Hashiguchi A, Nakamura T, Nozuma S, Sakiyama Y, Yoshimura A, Izumo S, Takashima H.	Hereditary Sensory and Autonomic Neuropathy Type IID caused by an SCN9A Mutation.	Neurology	80(18)	1641-9	2013
Yuan JH, Sakiyama Y, Higuchi I, Inamori Y, Higuchi Y, Hashiguchi A, Higashi K, Yoshimura A, Takashima H.	Mitochondrial myopathy with autophagic vacuoles in patients with the m.8344A>G mutation.	J Clin Pathol.			2013 Epub ahead of print

Yuan J, Higuchi Y, Nagado T, Nozuma S, Nakamura T, Matsuura E, Hashiguchi A, Sakiyama Y, Yoshimura A, Takashima H.	Novel mutation in the replication focus targeting sequence domain of DNMT1 causes hereditary sensory and autonomic neuropathy IE.	J Peripher Nerv Syst.	18(1)	89-93	2013
Yonekawa T, Komaki H, Saito Y, Takashima H, Sasaki M.	Congenital hypomyelinating neuropathy attributable to a de novo p.Asp61Asn mutation of the myelin protein zero gene.	Pediatr Neurol.	48(1)	59-62	2013
Arimura A, Deguchi T, Sugimoto K, Uto T, Nakamura T, Arimura Y, Arimura K, Yagihashi S, Nishio Y, Takashima H.	Intraepidermal nerve fiber density and nerve conduction study parameters correlate with clinical staging of diabetic polyneuropathy.	Diabetes Res Clin Pract.	99(1)	24-9	2013
Miki Y, Tomiyama M, Haga R, Nishijima H, Suzuki C, Kurihara A, Sugimoto K, Hashiguchi A, Takashima H, Baba M.	A family with IVIg-responsive Charcot-Marie-Tooth disease.	J Neurol.	260(4)	1147-5111	2013
Zhao Z, Hu J, Sakiyama Y, Okamoto Y, Higuchi I, Li N, Shen H, Takashima H.	DYSF mutation analysis in a group of Chinese patients with dysferlinopathy.	Clin Neurol Neurosurg.			2012 Epub ahead of print
Nakamura T, Hashiguchi A, Suzuki S, Uozumi K, Tokunaga S, Takashima H.	Vincristine exacerbates asymptomatic Charcot-Marie-Tooth disease with a novel EGR2 mutation.	Neurogenetics	13 (1):	77- 81	2012

Iguchi M, Hashiguchi A, Ito E, Toda K, Urano M, Shimizu Y, Takeuchi C, Saito K, Takashima H, Uchiyama S.	Charcot-marie-tooth disease type 4C in Japan: report of a case.	Muscle Nerve	47(2)	283-286	2012
Tokunaga S, Hashiguchi A, Yoshimura A, Maeda K, Suzuki T, Haruki H, Nakamura T, Okamoto Y, Takashima H.	Late-onset Charcot-Marie-Tooth disease 4F caused by periaxin gene mutation.	Neurogenetics	13(4)	359-65	2012
Shiga K, Noto Y, Mizuta I, Hashiguchi A, Takashima H, Nakagawa M.	A novel EGR2 mutation within a family with a mild demyelinating form of Charcot-Marie-Tooth disease.	J Peripher Nerv Syst.	17(2)	206-9	2012
Kawabata T, Higashimoto I, Takashima H, Izumo S, Kubota R.	Human T-lymphotropic virus type I (HTLV-I)-specific CD8+ cells accumulate in the lungs of patients infected with HTLV-I with pulmonary involvement.	J Med Virol.	84(7)	1120-7	2012
Saiga T, Tateishi T, Torii T, Kawamura N, Nagara Y, Shigeto H, Hashiguchi A, Takashima H, Honda H, Ohyagi Y, Kira J.	Inflammatory radiculoneuropathy in an ALS4 patient with a novel SETX mutation.	J Neurol Neurosurg Psychiatry.	83(7)	763-4	2012
Inamori Y, Higuchi I, Inoue T, Sakiyama Y, Hashiguchi A, Higashi K, Shiraishi T, Okubo R, Arimura K, Mitsuyama Y, Takashima H.	Inclusion body myositis coexisting with hypertrophic cardiomyopathy: an autopsy study.	Neuromuscul Disord.	22(8)	747-54	2012

Zhao Z, Hashiguchi A, Hu J, Sakiyama Y, Okamoto Y, Tokunaga S, Zhu L, Shen H, Takashima H.	Alanyl-tRNA synthetase mutation in a family with distal hereditary motor neuropathy.	Neurology	78(21)	1644-9	2012
Hasui K, Wang J, Tanaka Y, Izumo S, Eizuru Y, Matsuyama T.	Development of ultra-super sensitive immune-histochemistry and its application to the etiological study of adult T-cell leukemia/lymphoma.	Acta Histochem Cytochem.	45(2)	83-106	2012
出雲周二	HTLV-1 感染症で起こる疾患－白血病・HAM など。HTLV-1 母児感染予防のための基礎知識。特集 クローズアップ感染症。	小児内科	44(7)	973-977	2012
出雲周二	HAM の最新の話	Neuroinfection.	17(1)	6-10	2012
Ishiura H, Sako W, Yoshida M, Nakagawa M, Kaji R, Tsuji S, et al.	The TRK-fused gene is mutated in hereditary motor and sensory neuropathy with proximal dominant involvement.	Am J Hum Genet.	91	320-329	2012
中川正法	Charcot-Marie-Tooth 病 1.病態・治療。	最新医学 別冊 新しい診断と治療のABC75 末梢神経障害		152-160	2012
Shiga K, Noto Y, Mizuta I, Hashiguchi A, Takashima H, Nakagawa M.	A novel EGR2 mutation within a family with a mild demyelinating form of Charcot-Marie-Tooth disease.	J Periph Nerv Syst.	17	206-209	2012
Shiga K, Tsuji Y, Fujii C, Noto Y, Nakagawa M.	Demyelinating features in sensory nerve conduction in Fisher syndrome.	Intern Med.	51	2307-12	2012
Shiga K, Tanaka E, Isayama R, Mizuno T, Itoh K, Nakagawa M.	Chronic inflammatory demyelinating polyneuropathy due to administration of pegylated interferon- α 2b:a neuropathological case report.	Intern Med.	51	217-221	2012
Kawabata T, Higashimoto I, Takashima H, Izumo S, Kubota R.	Human T-lymphotropic virus type I (HTLV-I)-specific CD8+ cells accumulate in the lungs of patients infected with HTLV-I with pulmonary involvement.	J Med Virol.	84(7)	1120-7	2012
久保田龍二	HAM スペクトラム	神経内科	77	283-8	2012

Tanaka F, Katsuno M, Banno H, Suzuki K, Adachi H, Sobue G.	Current status of treatment of spinal and bulbar muscular atrophy.	Neural Plast.	2012	369284	2012
Tanaka F, Ikenaka K, Yamamoto M, Sobue G. Neuropathology and omics in motor neuron diseases.	Neuropathology and omics in motor neuron diseases.	Neuropathology	32(4)	458-446	2012
Iida M, Koike H, Ando T, Sugiura M, Yamamoto M, Tanaka F, Sobue G.	A novel MPZ mutation in Charcot-Marie-Tooth disease type 1B with focally folded myelin and multiple entrapment neuropathies.	Neuromuscul Disord.	22(2)	166-169	2012
田中章景、曾根淳、熱田直樹、中村亮一、土井 宏、児矢野 繁、祖父江 元	ALS のパーソナルゲノム解析	BRAIN and NERVE	65(3)	257-265	2013
Tamai Y., Hasegawa A., Takamori A., Sasada A., Tanosaki R., Choi I., Utsunomiya A., Maeda Y., Yamano Y., Eto T., Koh K., Nakamae H., Suehiro Y., Kato K., Takemoto S., Okamura J., Uike N., Kannagi M.	Potential contribution of a novel Tax epitope-specific CD4+ T cells to graft versus-Tax effects in adult T-cell leukemia patients after allogeneic hematopoietic stem cell transplantation	Journal of Immunology	in press		2013
Yamano Y., Sato T.	Clinical pathophysiology of human T-lymphotropic virus-type1-associated myelopathy/tropical spastic paraparesis.	Frontiers in Microbiology	3(389)	1-10	2012
山野嘉久、佐藤知雄	HTLV-1 関連脊髄症 (HAM) の病態・治療とバイオマーカー	日本臨牀	71(5)	in press	2013

山野嘉久、佐藤知雄、宇都宮與	HTLV-1 関連脊髄症 (HAM)	日本臨牀	in press		2013
山野嘉久、佐藤知雄、安藤仁、新谷奈津美、八木下尚子	HTLV-1 関連脊髄症 (HAM) の治療法を確立していくために—その現状と展望	日本臨牀	70(4)	705-713	2012
Brian Yao, Francesca Bagnato, Eiji Matsuura, Hellmut Merkle, Peter van Gelderen, Frederic K. Cantor, Jeff H. Duyn	Chronic Multiple Sclerosis Lesions: Characterization with High-Field-Strength MR imaging.	Radiology	262(1)	206-15	2012
Yoshimi Enose-Akahata, Eiji Matsuura, Yuetsu Tanaka, Unsung Oh, Steven Jacobson	Minocycline modulates antigen-specific CTL activity through inactivation of mononuclear phagocytes in patients with HTLV-I associated neurologic disease.	Retrovirology	9:16	1-14	2012
松浦英治、久保田龍二、樋口逸郎	HTLV-1 と筋炎	Clinical Neuroscience	30(3)	322-333	2012

IV. 研究成果の刊行物・別刷

Hereditary sensory and autonomic neuropathy type IID caused by an *SCN9A* mutation

Junhui Yuan, MD
Eiji Matsuura, MD, PhD
Yujiro Higuchi, MD
Akihiro Hashiguchi, MD
Tomonori Nakamura,
MD, PhD
Satoshi Nozuma, MD
Yusuke Sakiyama, MD,
PhD
Akiko Yoshimura, BS
Shuji Izumo, MD
Hiroshi Takashima, MD,
PhD

Correspondence to
Dr. Takashima:
thiroshi@m3.kufm.kagoshima-u.ac.jp

ABSTRACT

Objective: To identify the clinical features of Japanese patients with suspected hereditary sensory and autonomic neuropathy (HSAN) on the basis of genetic diagnoses.

Methods: On the basis of clinical, in vivo electrophysiologic, and pathologic findings, 9 Japanese patients with sensory and autonomic nervous dysfunctions were selected. Eleven known HSAN disease-causing genes and 5 related genes were screened using a next-generation sequencer.

Results: A homozygous mutation, c.3993delGinsTT, was identified in exon 22 of *SCN9A* from 2 patients/families. The clinical phenotype was characterized by adolescent or congenital onset with loss of pain and temperature sensation, autonomic nervous dysfunctions, hearing loss, and hyposmia. Subsequently, this mutation was discovered in one of patient 1's sisters, who also exhibited sensory and autonomic nervous system dysfunctions, with recurrent fractures being the most predominant feature. Nerve conduction studies revealed definite asymmetric sensory nerve involvement in patient 1. In addition, sural nerve pathologic findings showed loss of large myelinated fibers in patient 1, whereas the younger patient showed normal sural nerve pathology.

Conclusions: We identified a novel homozygous mutation in *SCN9A* from 2 Japanese families with autosomal recessive HSAN. This loss-of-function *SCN9A* mutation results in disturbances in the sensory, olfactory, and autonomic nervous systems. We propose that *SCN9A* mutation results in the new entity of HSAN type IID, with additional symptoms including hyposmia, hearing loss, bone dysplasia, and hypogeusia. *Neurology*® 2013;80:1641-1649

GLOSSARY

CIP = channelopathy-associated insensitivity to pain; **CMAP** = compound muscle action potentials; **HSAN** = hereditary sensory and autonomic neuropathy; **Nav1.7** = voltage-gated sodium channel; **dbSNP** = single nucleotide polymorphism database; **SCV** = sensory nerve conduction velocity; **SCN9A** = sodium channel, voltage-gated, type 9, α ; **SNAP** = sensory nerve action potentials.

Hereditary sensory and autonomic neuropathy (HSAN) is a clinically and genetically heterogeneous group of disorders. Until now, HSAN has been classified into 6 main groups on the basis of their mode of inheritance and clinical features, and 11 HSAN disease-causing genes have been identified (table 1¹⁻¹⁷).

SCN9A encodes the voltage-gated sodium channel (Nav1.7), and the gain-of-function mutations result in several painful disorders, including inherited erythromelalgia,¹⁸ paroxysmal extreme pain disorder,¹⁹ and small nerve fiber neuropathy.²⁰ Loss-of-function *SCN9A* mutations have been linked to channelopathy-associated insensitivity to pain (CIP), which is characterized by congenital insensitivity to pain perception and anosmia; however, the autonomic dysfunction has been regarded as exclusionary criteria for the diagnosis of CIP.²¹ It is noteworthy that no definite abnormalities have been recorded using either nerve conduction studies or sural nerve pathologic examinations in all of the previous cases with homozygous loss-of-function *SCN9A* mutations and part with compound heterozygous mutations.²²⁻²⁶ However, a slight reduction in sensory nerve action potentials (SNAP) was recorded in two cases with compound heterozygous *SCN9A* mutations.^{25,27}

Supplemental data at
www.neurology.org

From the Department of Neurology and Geriatrics (J.Y., E.M., Y.H., A.H., T.N., S.N., Y.S., A.Y., H.T.), Kagoshima University, Graduate School of Medical and Dental Sciences, Kagoshima; and Department of Molecular Pathology (S.I.), Center for Chronic Viral Diseases, Kagoshima University School of Medicine, Kagoshima, Japan.

Go to Neurology.org for full disclosures. Funding information and disclosures deemed relevant by the authors, if any, are provided at the end of the article.

Table 1 Overview of HSAN disease-causing genes, inheritance pattern, and cardinal phenotypic features

Gene symbol	HSAN type	Inh	Onset age	Cardinal clinical features
<i>SPTLC1</i>	IA	AD	Adulthood	Loss of pain and temperature sensation; occasional autonomic involvement; variable sensorineural deafness and distal motor involvement ^{1,2}
<i>SPTLC2</i>	IC	AD		
<i>ATL1</i>	ID	AD	Early adulthood	Severe loss of pain, temperature, and vibration sensation; ulcero-mutilation; spastic paraparesis; rare autonomic involvement ³
<i>DNMT1</i>	IE	AD	Childhood-adulthood	Severe sensory loss; ulcero-mutilation; sensorineural hearing loss; early-onset dementia; no autonomic symptoms ⁴⁻⁶
<i>WNK1</i>	IIA	AR	Congenital—early childhood	Severe distal loss of touch, pain, and temperature sensation; mutilations in hands and feet; mild or asymptomatic autonomic dysfunction ^{7,8}
<i>FAM134B</i>	IIB	AR	Childhood	Severe loss of pain and temperature sensation; ulcero-mutilation; autonomic dysfunctions ⁹
<i>KIF1A</i>	IIC	AR	Childhood	Severe loss of pain, temperature, vibration, and position sensation; ulcero-mutilation; distal muscle weakness; developmental delay and short stature ¹⁰
<i>IKBKAP</i>	III	AR	Congenital	Familial dysautonomia; gastrointestinal and respiratory dysfunction; scoliosis; relative indifference to pain and temperature ¹¹⁻¹³
<i>NTRK1</i>	IV	AR	Congenital—early childhood	Loss of pain and temperature sensation; anhidrosis; episodic fever; mild mental retardation; joint deformities ¹⁴
<i>NGF</i>	V	AR	Congenital—adulthood	Reduced sensation of pain and temperature; variable autonomic dysfunctions; painless fractures; joint deformities; mild mental retardation ^{15,16}
<i>DST</i>	VI	AR	Congenital	Dysautonomia; hypotonia; facial deformity; decreased pain response; joint contractures; retardation; respiratory failure; early death ¹⁷

Abbreviations: AD = autosomal dominant; AR = autosomal recessive; *ATL1* = atlastin GTPase 1; *DNMT1* = DNA (cytosine-5)-methyltransferase 1; *DST* = dystonin; *FAM134B* = family with sequence similarity 134, member B; *IKBKAP* = inhibitor of κ light polypeptide gene enhancer in B cells, kinase complex-associated protein; Inh = inheritance; *KIF1A* = kinesin family member 1A; *NGF* = nerve growth factor (β polypeptide); *NTRK1* = neurotrophic tyrosine kinase, receptor, type 1; *SPTLC1* = serine palmitoyltransferase, long chain base subunit 1; *SPTLC2* = serine palmitoyltransferase, long chain base subunit 2; *WNK1* = WNK lysine deficient protein kinase 1.

In this study, using a next-generation sequencer, in 9 Japanese patients who were diagnosed with HSAN based on their clinical, in vivo electrophysiologic, and pathologic features, 11 known HSAN disease-causing genes and 5 related genes including *SCN9A* were screened. We identified a homozygous frameshift mutation in *SCN9A* of 2 patients/families. Therefore, we demonstrate that loss-of-function *SCN9A* mutation can produce a typical HSAN phenotype, and we propose this new classification as HSAN type IID. This study also broadened the spectrum of clinical phenotypes in patients with *SCN9A*-related disorders. Furthermore, on the basis of clinical, in vivo electrophysiologic, and pathologic findings, we attempted to elucidate the pathogenesis of the mutated $\text{Na}_v1.7$.

METHODS All patients who were referred to our department from 2000 to 2012 and who had sensory and autonomic nerve dysfunctions were selected. After excluding patients who had

associated multiple motor nerve involvement, 9 patients were enrolled and genotyped in this study. Besides the 11 known HSAN disease-causing genes described above, we also investigated another 5 genes that might also cause sensory and autonomic symptoms, including *SCN9A*, *CCT5*, *PRNP*, *FLVCR1*, and *RNF170*.

The protocol of the following study was reviewed and approved by the Institutional Review Board of Kagoshima University. All patients and family members provided written informed consent to participate in this study.

Pathologic study. Sural nerve biopsies, performed at the age of 42 years in patient 1 and at the age of 25 years in patient 2, were analyzed according to standard morphologic procedures for light and electron microscopy.²⁸ A portion of the specimen was prepared for teased fiber analysis and classified according to Dyck's criteria.²⁹ The diameter and density of the myelinated fibers were analyzed with a Luzex AP image analyzer (Nireco Corporation, Tokyo, Japan).

Mutation sequencing. Genomic DNA was extracted from the peripheral blood leukocytes.

Using the Primer 3 program, we designed 375 oligonucleotide primers that covered all 357 coding exons and exon-intron junctions with amplicon lengths of 400–500 base pairs. Briefly, all target fragments of 9 patients were amplified by multiplex PCR (QIAGEN Multiplex PCR Kit; QIAGEN GmbH, Hilden, Germany) and ligated with specified indexes, respectively, then screened on the MiSeq sequencing system simultaneously in

accordance with the manufacturer's protocol. The results were mapped to the genome reference sequence in the CLC Genomics Workbench 4 (CLC Bio, Aarhus, Denmark) and then analyzed with tablet software.³⁰

The polymorphic and pathogenic natures of the confirmed variants were checked against the single nucleotide polymorphism database (dbSNP) (<http://www.ncbi.nlm.nih.gov/snp/>) and the 1000 Genomes database (<http://browser.1000genomes.org/index.html>). To confirm the suspected pathogenic mutations or low coverage domains (depth less than 10) in the MiSeq sequencing output, Sanger sequencing was also performed using the same methodology as the one employed in a previous study.³¹ We screened 100 Japanese population control patients for the c.3993delGinsTT mutation.

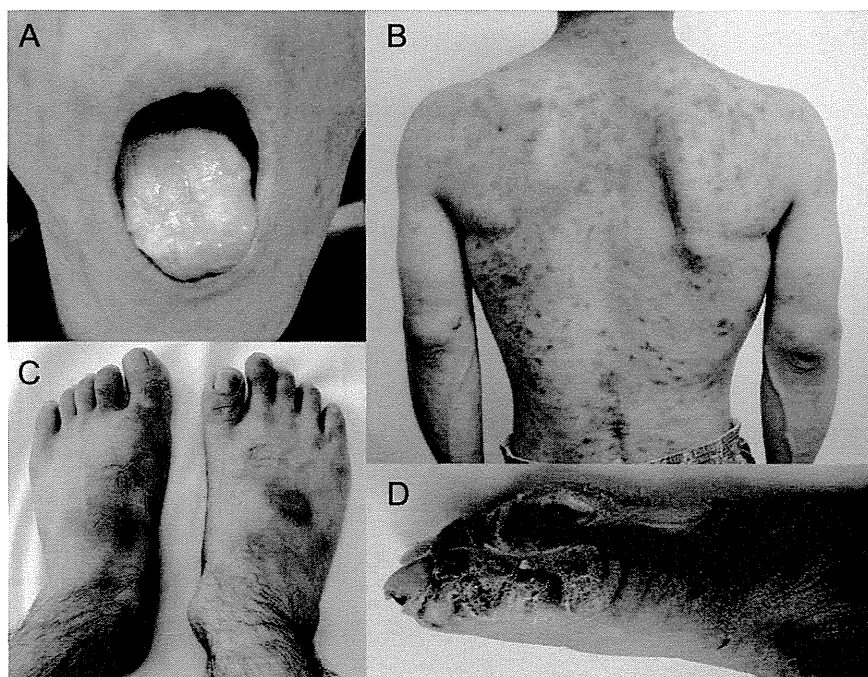
RESULTS Patients. Patient 1. This 50-year-old man was the sixth child from a consanguineous family. No abnormalities were noted at birth or in the early developmental stages except for slight hyposmia since childhood. Since primary school, pain perception started to decrease in his hands and feet. At 30 years of age, he underwent lumbar spinal fixation, but felt no pain. After 40 years of age, the numbness progressed from the distal to the proximal limbs. Furthermore, his toes could not perceive temperature well when he entered his bath, and while walking, his right slipper always slipped off. There was no history of episodes of unexplained vomiting or dysphagia. A detailed physical examination revealed multiple skin lesions, including a burn mark on the right middle finger, which was caused by a cigarette. No pupillary abnormalities were observed. His muscle strength was normal, except

grade 4+/5 weakness in the right tibialis anterior muscle. He also had a slight steppage gait. All reflexes were diminished, and his pathologic reflexes were negative. Pain and temperature perception were reduced in the distal limbs and absent in his feet. However, sense of vibration, joint position, and pressure were all preserved. Postural hypotension was excluded. During the sweating test, no sweating was observed in his face or any of his limbs, except in the palm of his left hand. Asymptomatic sensorineural hearing loss with an increase in the 4,000-Hz threshold in the left ear was diagnosed by an otorhinolaryngologist. MRI of the brain was normal.

In nerve conduction study, all motor nerve conduction velocity and compound muscle action potentials (CMAP) values were normal, except for a slightly reduced CMAP in the right tibial nerve at 3.5 mV (normal range, >4.4 mV). Sensory nerve conduction velocity (SCV) was slightly slow in the right median and ulnar nerve at 45.2 m/s (normal range, >47.2 m/s) and 40 m/s (normal range, >46.9 m/s), respectively, and moderately slow in the right sural nerve at 27.5 m/s (normal range, >40.8 m/s). SNAP amplitudes were markedly reduced in the right median nerve (0.9 μ V; normal range, >7.0 μ V), bilateral ulnar nerves (1.3 and 2.2 μ V; normal range, >6.9 μ V), and the right sural nerves (1.0 μ V; normal range, >5.0 μ V). However, the SCV and SNAP in the left median nerve were normal.

Patient 2. This 33-year-old man was from a nonconsanguineous family having no history of neurologic

Figure 1 Clinical pictures of patient 2



(A) Reduced number of fungiform papilla on the tongue. (B) The back of patient 2, showing scattered rash, pigmentation, and short humerus. (C) Short right hallux. (D) Multiple painless ulcers and deformed joints in the fingers.

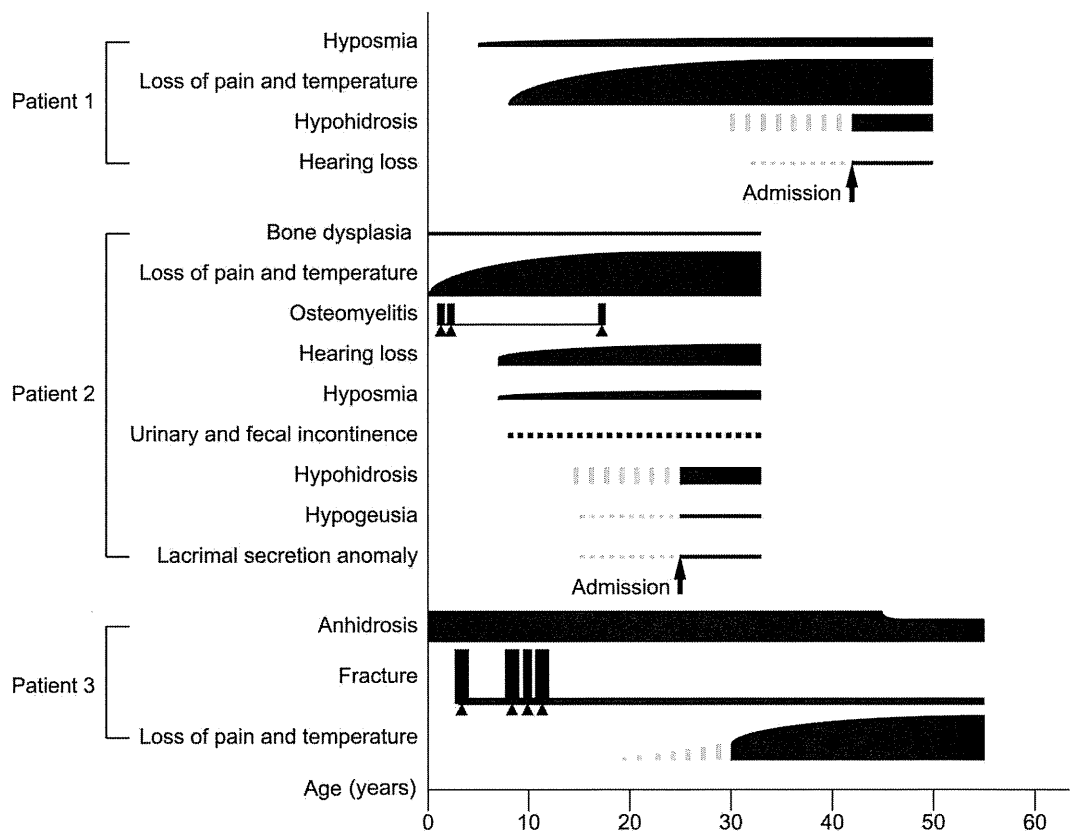
disorders. Decreased pain and temperature perception was noted at birth. When he was a year old, his feet were burnt after he walked on asphalt on a hot summer day, and this eventually progressed to osteomyelitis. Subsequently, he underwent operations of the right tibia and both feet, but he could not feel any pain. Before enrolling in primary school, hearing loss in the left ear and hyposmia were detected. He experienced occasional urinary and fecal incontinence, and frequent urination at night. His height was 157 cm, and he had a short humerus (27.5 cm) and right hallux (figure 1, B and C). Left acetabular dysplasia was noticed, which contributed to his left lower limb being 3 cm longer than his right lower limb. Rash and pigmentation were scattered over his chest and back (figure 1B), and several painless ulcers and deformed joints were observed in his fingers (figure 1D). Tendon hyperreflexia was noted in the lower limbs, and pathologic reflexes were negative. Pain perception was impaired in a glove–stocking pattern. Sense of vibration, joint position, and pressure were all normal. The sweating test revealed reduced sweating tendency throughout the body and especially in the trunk, except for his hands and feet. Postural hypotension was excluded, and brain MRI was normal. A lacrimal secretion anomaly was also detected. Otorhinolaryngologic examinations revealed the following:

deafness in the left ear and minimal hearing loss in the right ear, glossopharyngeal and chorda tympani nerve abnormalities in the gustatory sensation test, reduced number of fungiform papilla on his tongue (figure 1A), and a decline in olfactory acuity as tested by a jet stream olfactometer. Examinations of the urinary tract excluded any organic disease.

The nerve conduction study revealed all motor nerve conduction velocity and CMAP values within normal ranges. The SCV was slightly slow in the right median and ulnar nerves (45.2 m/s and 46.2 m/s, respectively). However, SNAP was moderately decreased in the bilateral median (7 and 5.7 μ V) and ulnar (3.3 and 4.4 μ V) nerves. Nevertheless, no abnormalities were detected in sural nerve SCV and SNAP values.

Patient 3. This 55-year-old woman was an elder sister of patient 1. Her pregnancy was uneventful and delivery was normal. She had recurrent fractures and underwent operations for the left thigh (at age of 3 years and 8 years), right thigh (at age 11 years), and left elbow (primary school). When she was 30 years old, she perceived no pain after her feet were burnt on a heater. Anhidrosis was also noted, but after the age of 45 years, occasional sweat was secreted on her back. There was no evident hyposmia or hearing loss. At present, she is able to stand up and walk using

Figure 2 Clinical courses of the 3 patients



The solid triangles (▲) indicate surgery.

her hands for support. Cranial nerve examinations were normal. Deformities of the left elbow, right foot, and bilateral lower limbs were noted. Muscle strength testing was normal in the upper limbs, whereas the strength in the lower limb muscles decreased to grades 2/5–4/5. Pain and temperature perceptions were reduced in the distal lower limbs and the anterior part of the right thigh, which may have been involved because of damage from surgery. The sense of vibration and joint position were preserved. Reflexes in her lower limbs were absent, and her pathologic reflexes were negative. Osteoporosis was excluded by an orthopedist.

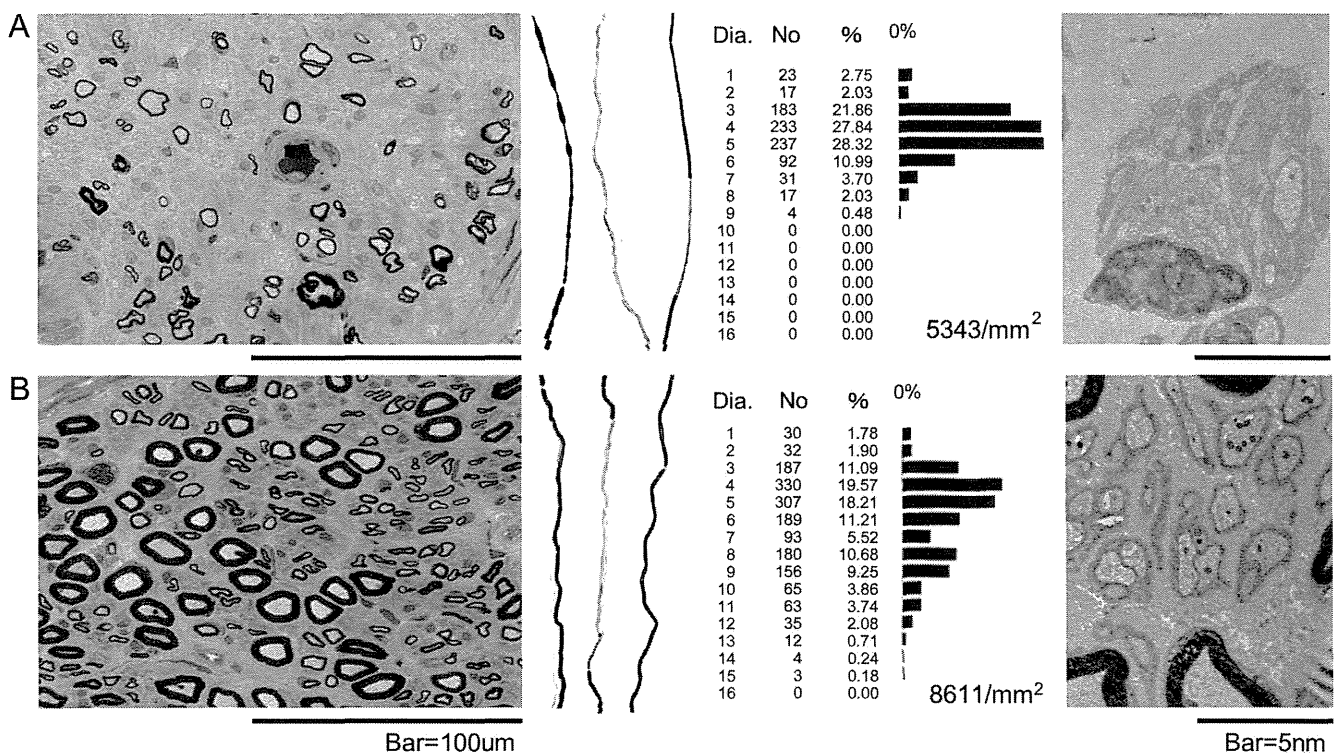
The clinical courses of the 3 patients described above, including the onset and imaged severities of each symptom, are shown in figure 2.

Pathologic studies. In patient 1, the number of myelinated fibers was markedly decreased in all fasciculi, but the changes varied in their scale and extent. A histogram of the fiber diameter indicated a marked loss of large myelinated fibers relative to small myelinated fibers. Some remaining myelinated fibers had thinner myelin sheaths and some exhibited axonal degeneration. An electron microscopic study revealed clusters of Schwann cell processes, which may have been caused by the axonal degeneration of unmyelinated

fibers (figure 3A). Contrary to the findings in patient 1, the number of myelinated fibers in patient 2 was slightly decreased, even with marked clinical symptoms. The histogram of fiber diameter showed a normal pattern. Electron microscopy showed that unmyelinated fibers were fairly preserved (figure 3B). No demyelinated fibers or inflammatory cells could be found in either patient.

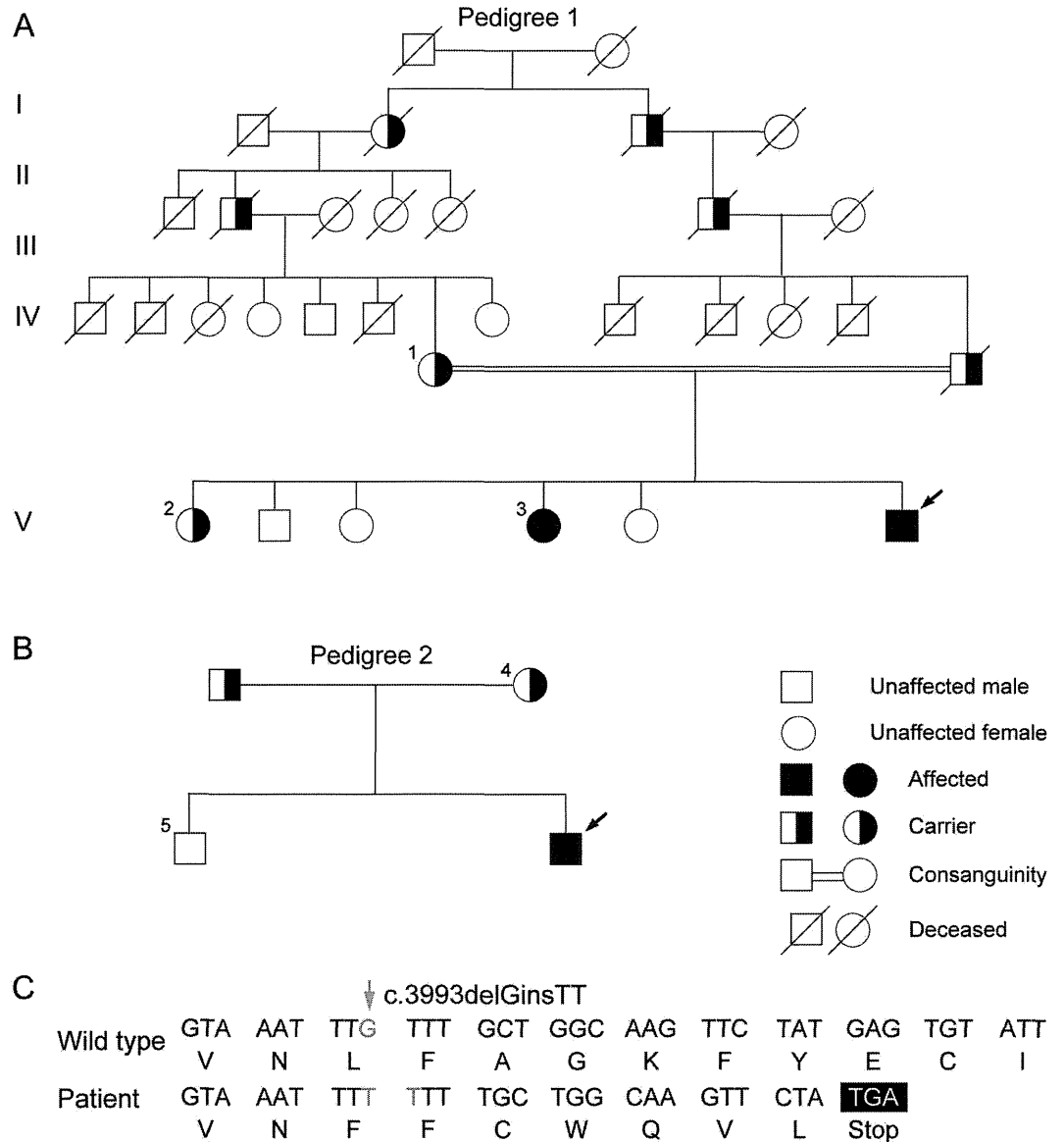
Genetic studies. Using the MiSeq sequencing system, all of the 9 patients were genotyped successfully. Besides patients 1 and 2, no pathogenic mutation was detected. The CLCbio software showed that 96.24% and 93.6% of the data matched the reference sequences in patients 1 and 2, respectively. In the 357 targeted exons, 98.04% and 97.76% covered more than 10 reads. From patients 1 and 2, a total of 41 high-confidence variants were detected (table e-1 on the *Neurology*[®] Web site at www.neurology.org). In these variants, 39 known SNPs were coincident with the dbSNP or 1000 Genome database. Of the remaining 2 variants, the c.3248A>C in *KIF1A* was found in normal controls and was therefore considered as an SNP. A homozygous mutation in exon 22 of *SCN9A*, c.3993delGinsTT, remained. This mutation was not observed in 100 Japanese control patient samples,

Figure 3 Pathologic findings from the sural nerve biopsies



In patient 1, the density of large and small myelinated fibers is markedly decreased. The remaining myelinated fibers have thinner myelin sheaths. Some teased fibers exhibit axonal degeneration. The histogram of the fiber diameter indicates loss of large myelinated fibers (5,343 fibers/mm²). Electron microscopic examination shows clusters of Schwann cell processes (A). In patient 2, the densities of large and small myelinated fibers are slightly decreased. Teased fibers exhibit shortened internodal remyelination. The histogram of the fiber diameter shows a normal pattern (8,611 fibers/mm²). Unmyelinated fibers are fairly preserved, as shown under the electron microscope (B).

Figure 4 Pedigree diagram and genetic studies



(A) Pedigree of patient 1. Patients 1 and 3 (V3) harbor the homozygous mutation, c.3993delGinsTT, whereas their mother (IV1) and 1 elder sister (V2) are heterozygous carriers. (B) Pedigree of patient 2. The same mutation, c.3993delGinsTT, can be observed in patient 2. His mother (4) exhibits the carrier genotype, and his elder brother (5) is normal. The black arrows (↘) indicate the proband. All the family members with available DNA samples are labeled with an Arabic numeral. (C) The c.3993delGinsTT mutation (↓) shifts the reading frame and generates a premature stop codon.

nor did we find it on the 1000 Genomes Web site, which catalogs human genetic variations using 2,500 patient samples, including 500 East Asian (100 Japanese) patient samples. DNA samples were then collected from 3 other family members of pedigree 1, and 2 members of pedigree 2. In patient 3, the same genotype was identified. In addition, asymptomatic carriers (mother and another elder sister of patient 1 and the mother of patient 2) and an unaffected member (brother of patient 2) were found (figure 4, A and B). This mutation changes the reading frame during the translation of the mRNA and generates a premature stop codon (figure 4C).

DISCUSSION Among the 16 disease-causing or related genes of HSAN, we identified a homozygous mutation in *SCN9A* from 2 Japanese families. We described 3 patients who presented with new clinical, in vivo electrophysiologic, and pathologic phenotypes.

SCN9A, which is located on chromosome 2q24.3, contains 26 coding exons.³² It encodes Na_v1.7, which is the α-subunit of a tetrodotoxin-sensitive, voltage-gated sodium channel. Na_v1.7, composed of 4 domains, each with 6 transmembrane domains and 2 highly conserved pore-forming segments,³³ is preferentially expressed within the dorsal root ganglion and sympathetic ganglion neurons and their small-diameter peripheral

axons.³⁴ It is crucial for the depolarizing phase of neuronal action potentials, and it seems to determine the excitability and repetitive firing properties of neurons.³⁵ Gain-of-function *SCN9A* mutations result in hyperexcitable nociceptive neurons and states, such as inherited erythromelalgia,¹⁸ paroxysmal extreme pain disorder,¹⁹ and small nerve fiber neuropathy,²⁰ whereas loss-of-function *SCN9A* mutations produce no sodium current and generate CIP.²²

In our study, both families lived in the Kagoshima prefecture, which is located to the south of Kyushu Island, Japan, and both were unrelated to each other. Loss of pain and temperature perceptions began at different ages, appearing as early as birth in patient 2, in the second decade in patient 1, and in the third decade in patient 3. Their ages at the onset of symptoms were different from those reported for patients with CIP who had a congenital onset. Moreover, in these 3 patients, the area of their pain insensitivities was limited mainly within the distal part of the limbs, not the entire body, as is seen in patients with CIP. The sense of vibration and joint position were preserved in our patients. However, the predominant reduction in sweat production in our 3 patients, together with urination and defecation disorder, lacrimal secretion anomaly, and decreased number of fungiform papilla on the tongue in patient 2, suggested autonomic nervous system dysfunction. A recent study indicated that Na_v1.7 in sympathetic neurons also contributes to the sensation of neuropathic pain.³⁶ The severe rash and pigmentation may be due to a post-inflammatory hyperpigmentation, resulting from the disruption of autonomic innervation. Meanwhile, hyposmia/anosmia, which is a common feature in patients with CIP and loss-of-functional *SCN9A* mutation,^{23,27,37} was also identified in our patients. Furthermore, in patient 2, hypogeusia was detected using a gustatory sensation test. Bone dysplasia, as an additional symptom in patient 2 (acetabular dysplasia, short humerus, and right hallux), had also been reported in a Dutch kindred.³⁸ The otorhinolaryngologist confirmed hearing loss, although at different levels, in patients 1 and 2, which has mainly been recorded in patients with HSAN type IE.⁴⁻⁶ These findings definitely broaden the symptomatic heterogeneity of *SCN9A* mutations.

Although pain insensitivity was symmetrically detected in the distal portion of the limbs of the 2 index patients, nerve conduction studies only revealed asymmetric involvement of the extremities. These findings, except those of the peroneal nerve, were compatible with sensory-predominant axonal multiple mononeuropathy complicated by minimal demyelinating changes, rather than a polyneuropathy.

Interestingly, the pathologic features of the sural nerve in the 2 index cases also varied. Although decreases in the small and large myelinated fibers were observed among the fasciculi in patient 1, the extent

was dramatically different, whereas the density of small and large myelinated fibers was fairly preserved in patient 2. These discoveries were consistent with the nerve conduction study findings, which suggested a mismatch between the distribution of affected fibers and the severity of the loss-of-pain sensations. In addition, especially in patient 1, both decreased large myelinated fibers and decreased SNAP/SCV indicated that the large myelinated fibers were affected, whereas cases with gain-of-function *SCN9A* mutations always present with small myelinated and unmyelinated fiber abnormalities.²⁰ The selective involvement of sensory nerves in these patients is inconsistent with the clinical features and may indicate that the dysfunction of the dorsal root ganglion is more predominant than that of the peripheral nerve. However, the mechanisms underlying the pathologic aberrations in the fasciculi or nerves, caused by the mutated Na_v1.7 in the dorsal root ganglion, require further research.

The homozygous mutation, c.3993delGinsTT, which is located in exon 22 of *SCN9A*, is expected to shift the reading frame from amino acid 1331 (p. leu1331phe) and generate a premature stop codon. This will induce an essential alteration in the fifth transmembrane segment of domain 3 in Na_v1.7 and eliminate the whole fourth domain. The nonsense-mediated messenger RNA decay mechanism will then be activated, which will induce loss of function of Na_v1.7 in nociceptive neurons. Together with the pedigree study that confirmed the cosegregation of the genotype and phenotype, this mutation was believed to be a pathogenic mutation.

In 3 patients from 2 Japanese families who experienced symptoms that were characterized by congenital or adolescence-onset loss of pain and temperature perception and autonomic nervous dysfunction accompanied by hyposmia, hearing loss, hypogeusia, bone dysplasia, and fractures, we identified a novel loss-of-function frameshift *SCN9A* mutation. We demonstrated that this was a new entity on the basis of clinical, in vivo electrophysiologic, and pathologic findings. We introduce this new entity as HSAN type IID, an allelic disorder with CIP, both of which result from loss-of-function mutations in *SCN9A*. Furthermore, on the basis of in vivo electrophysiologic and pathologic findings, we furthered the understanding of the mechanisms induced by the loss of function of Na_v1.7. We are able to summarize that a loss-of-function *SCN9A* mutation can produce heterogeneous phenotype, even harboring the same mutation.

AUTHOR CONTRIBUTIONS

Dr. Junhui Yuan: genetic study, analyses and interpretation of data, and drafting the manuscript. Dr. Eiji Matsuura: pathologic study of the sural nerve, analysis and interpretation of data, revising the manuscript. Dr. Yujiro Higuchi: acquisition and analysis of clinical data, revising the manuscript. Dr. Akihiro Hashiguchi: acquisition of clinical data

and case selection. Dr. Tomonori Nakamura: nerve conduction study, analysis and interpretation of data. Dr. Satoshi Nozuma: acquisition of clinical data. Dr. Yusuke Sakiyama and Ms. Akiko Yoshimura: participated in genetic study. Dr. Shuji Izumo: analysis and interpretation of data. Dr. Hiroshi Takashima: study concept and design, interpretation of the data, revising the manuscript, study supervision, obtain funding.

ACKNOWLEDGMENT

The authors thank Ms. Y. Shirahama and A. Nishibeppu of our department for their excellent technical assistance. They also thank the Joint Research Laboratory, Kagoshima University Graduate School of Medical and Dental Sciences, for the use of their facilities.

STUDY FUNDING

Supported by the Intramural Research Grant (23-5) for Neurological and Psychiatric Disorders of NCNP; Research Committee for Neuropathy, Ataxic Disease and Applying Health and Technology of Ministry of Health, Welfare and Labour, Japan; and a research grant (23300201) from the Ministry of Health, Labour, and Welfare of Japan.

DISCLOSURE

Drs. Yuan, Matsuura, Higuchi, Hashiguchi, Nakamura, Nozuma, Sakiyama, and Ms. Yoshimura report no disclosures. Dr. Izumo received an honorarium for lecturing from Bayer Japan, funded by grants from Research Committee for HAM and neuroimmunological diseases of the Ministry of Health, Welfare and Labour of Japan. Dr. Takashima served on the scientific advisory board for Teijin, received a royalty from Athena diagnostics, was on the speakers' bureaus of Astellas, Bayer Group, Kyowa Hakko Kirin Pharma, Takeda Pharmaceutical Company Limited, Biogen Idec, Novartis, Daiinippon Sumitomo Pharma, GlaxoSmithKline, Kowa Group, Pfizer Co., Mitsubishi Tanabe Pharma, and Eisai Co., is funded by grants from the Nervous and Mental Disorders and Research Committee for Ataxic Disease, Neuropathy, SMON, HAM, Chronic Pain, Applying Health and Technology of the Japanese Ministry of Health, Welfare and Labour, and received grants from Ministry of Education, Culture, Sports, Science, and Technology of Japan (grant 21591095). Go to Neurology.org for full disclosures.

Received November 2, 2012. Accepted in final form January 18, 2013.

REFERENCES

- Dawkins JL, Hulme DJ, Brahmabhatt SB, Auer-Grumbach M, Nicholson GA. Mutations in SPTLC1, encoding serine palmitoyltransferase, long chain base subunit-1, cause hereditary sensory neuropathy type I. *Nat Genet* 2001;27:309–312.
- Rotthier A, Auer-Grumbach M, Janssens K, et al. Mutations in the SPTLC2 subunit of serine palmitoyltransferase cause hereditary sensory and autonomic neuropathy type I. *Am J Hum Genet* 2010;87:513–522.
- Guelly C, Zhu PP, Leonardis L, et al. Targeted high-throughput sequencing identifies mutations in atlastin-1 as a cause of hereditary sensory neuropathy type I. *Am J Hum Genet* 2011;88:99–105.
- Wright A, Dyck PJ. Hereditary sensory neuropathy with sensorineural deafness and early-onset dementia. *Neurology* 1995;45:560–562.
- Hojo K, Imamura T, Takanashi M, et al. Hereditary sensory neuropathy with deafness and dementia: a clinical and neuroimaging study. *Eur J Neurol* 1999;6:357–361.
- Klein CJ, Botuyan MV, Wu Y, et al. Mutations in DNMT1 cause hereditary sensory neuropathy with dementia and hearing loss. *Nat Genet* 2011;43:595–600.
- Lafreniere RG, MacDonald ML, Dube MP, et al. Identification of a novel gene (HSN2) causing hereditary sensory and autonomic neuropathy type II through the Study of Canadian Genetic Isolates. *Am J Hum Genet* 2004;74:1064–1073.

- Coen K, Pareyson D, Auer-Grumbach M, et al. Novel mutations in the HSN2 gene causing hereditary sensory and autonomic neuropathy type II. *Neurology* 2006;66:748–751.
- Kurth I, Pamminger T, Hennings JC, et al. Mutations in FAM134B, encoding a newly identified Golgi protein, cause severe sensory and autonomic neuropathy. *Nat Genet* 2009;41:1179–1181.
- Rivière JB, Ramalingam S, Lavastre V, et al. KIF1A, an axonal transporter of synaptic vesicles, is mutated in hereditary sensory and autonomic neuropathy type 2. *Am J Hum Genet* 2011;89:219–230.
- Slaugenhaupt SA, Blumenfeld A, Gill SP, et al. Tissue-specific expression of a splicing mutation in the IKBKAP gene causes familial dysautonomia. *Am J Hum Genet* 2001;68:598–605.
- Anderson SL, Coli R, Daly IW, et al. Familial dysautonomia is caused by mutations of the IKAP gene. *Am J Hum Genet* 2001;68:753–758.
- Axelrod FB, Hilz MJ. Inherited autonomic neuropathies. *Semin Neurol* 2003;23:381–390.
- Mardy S, Miura Y, Endo F, et al. Congenital insensitivity to pain with anhidrosis: novel mutations in the TRKA (NTRK1) gene encoding a high-affinity receptor for nerve growth factor. *Am J Hum Genet* 1999;64:1570–1579.
- Einarsdottir E, Carlsson A, Minde J, et al. A mutation in the nerve growth factor beta gene (NGFB) causes loss of pain perception. *Hum Mol Genet* 2004;13:799–805.
- Carvalho OP, Thornton GK, Hertecant J, et al. A novel NGF mutation clarifies the molecular mechanism and extends the phenotypic spectrum of the HSN5 neuropathy. *J Med Genet* 2011;48:131–135.
- Edvardson S, Cinnamon Y, Jalas C, et al. Hereditary sensory autonomic neuropathy caused by a mutation in dystonin. *Ann Neurol* 2012;71:569–572.
- Yang Y, Wang Y, Li S, et al. Mutations in SCN9A, encoding a sodium channel alpha subunit, in patients with primary erythralgia. *J Med Genet* 2004;41:171–174.
- Fertleman CR, Baker MD, Parker KA, et al. SCN9A mutations in paroxysmal extreme pain disorder: allelic variants underlie distinct channel defects and phenotypes. *Neuron* 2006;52:767–774.
- Faber CG, Hoeijmakers JG, Ahn HS, et al. Gain of function Nav1.7 mutations in idiopathic small fiber neuropathy. *Ann Neurol* 2012;71:26–39.
- Goldberg YP, Pimstone SN, Namdari R, et al. Human Mendelian pain disorders: a key to discovery and validation of novel analgesics. *Clin Genet* 2012;82:367–373.
- Cox JJ, Reimann F, Nicholas AK, et al. An SCN9A channelopathy causes congenital inability to experience pain. *Nature* 2006;444:894–898.
- Goldberg YP, MacFarlane J, MacDonald ML, et al. Loss-of-function mutations in the Nav1.7 gene underlie congenital indifference to pain in multiple human populations. *Clin Genet* 2007;71:311–319.
- Ahmad S, Dahllund L, Eriksson AB, et al. A stop codon mutation in SCN9A causes lack of pain sensation. *Hum Mol Genet* 2007;16:2114–2121.
- Cox JJ, Sheynin J, Shorer Z, et al. Congenital insensitivity to pain: novel SCN9A missense and in-frame deletion mutations. *Hum Mutat* 2010;31:e1670–e1686.
- Staud R, Price DD, Janicke D, et al. Two novel mutations of SCN9A (Nav1.7) are associated with partial congenital insensitivity to pain. *Eur J Pain* 2011;15:223–230.

27. Nilsen KB, Nicholas AK, Woods CG, et al. Two novel SCN9A mutations causing insensitivity to pain. *Pain* 2009;143:155–158.
28. Schröder JM. Developmental and pathological changes at the node and paranode in human sural nerves. *Microsc Res Tech* 1996;34:422–435.
29. Dyck PJ, Giannini C, Lais A. Pathologic alterations of nerves. In: Dyck PJ, Thomas PK, Griffin JW, Low PA, Poduslo JF, editors. *Peripheral Neuropathy*, vol. 1, 3rd ed. Philadelphia: W.B. Saunders; 1993:514–595.
30. Milne I, Bayer M, Cardle L, et al. Tablet—next generation sequence assembly visualization. *Bioinformatics* 2010;26:401–402.
31. Okamoto Y, Higuchi I, Sakiyama Y, et al. A new mitochondria-related disease showing myopathy with episodic hypercreatinine kinase-emia. *Ann Neurol* 2011;70:486–492.
32. Michiels JJ, te Morsche RH, Jansen JB, Drenth JP. Autosomal dominant erythralgia associated with a novel mutation in the voltage-gated sodium channel alpha subunit Nav1.7. *Arch Neurol* 2005;62:1587–1590.
33. Klugbauer N, Lacinova L, Flockerzi V, Hofmann F. Structure and functional expression of a new member of the tetrodotoxin-sensitive voltage-activated sodium channel family from human neuroendocrine cells. *EMBO J* 1995;14:1084–1090.
34. Sangameswaran L, Fish LM, Koch BD, et al. A novel tetrodotoxin-sensitive, voltage-gated sodium channel expressed in rat and human dorsal root ganglia. *J Biol Chem* 1997;272:14805–14809.
35. Rush AM, Dib-Hajj SD, Liu S, Cummins TR, Black JA, Waxman SG. A single sodium channel mutation produces hyper- or hypoexcitability in different types of neurons. *Proc Natl Acad Sci USA* 2006;103:8245–8250.
36. Minett MS, Nassar MA, Clark AK, et al. Distinct Nav1.7-dependent pain sensations require different sets of sensory and sympathetic neurons. *Nat Commun* 2012;3:791.
37. Weiss J, Pyrski M, Jacobi E, et al. Loss-of-function mutations in sodium channel Nav1.7 cause anosmia. *Nature* 2011;472:186–190.
38. Hoeijmakers JG, Han C, Merkies IS, et al. Small nerve fibres, small hands and small feet: a new syndrome of pain, dysautonomia and acromesomelia in a kindred with a novel Nav1.7 mutation. *Brain* 2012;135:345–358.

Share Your Artistic Expressions in *Neurology* ‘Visions’

AAN members are urged to submit medically or scientifically related artistic images, such as photographs, photomicrographs, and paintings, to the “Visions” section of *Neurology*[®]. These images are creative in nature, rather than the medically instructive images published in the *NeuroImages* section. The image or series of up to six images may be black and white or color and must fit into one published journal page. Accompanying description should be 100 words or less; the title should be a maximum of 96 characters including spaces and punctuation.

Learn more at www.aan.com/view/Visions, or upload a Visions submission at submit.neurology.org.

Save These Dates for AAN CME Opportunities!

Mark these dates on your calendar for exciting continuing education opportunities, where you can catch up on the latest neurology information.

Regional Conference

- October 25-27, 2013, Las Vegas, Nevada, Encore at Wynn Hotel

AAN Annual Meeting

- April 26-May 3, 2014, Philadelphia, Pennsylvania, Pennsylvania Convention Center

Mitochondrial myopathy with autophagic vacuoles in patients with the m.8344A>G mutation

Jun-Hui Yuan, Yusuke Sakiyama, Itsuro Higuchi, Yukie Inamori, Yujiro Higuchi, Akihiro Hashiguchi, Keiko Higashi, Akiko Yoshimura, Hiroshi Takashima

► Additional material is published online only. To view please visit the journal online (<http://dx.doi.org/10.1136/jclinpath-2012-201431>).

Department of Neurology and Geriatrics, Kagoshima University, Graduate School of Medical and Dental Sciences, Kagoshima, Japan

Correspondence to

Dr Hiroshi Takashima, Department of Neurology and Geriatrics, Kagoshima University, Graduate School of Medical and Dental Sciences, 8-35-1 Sakuragaoka, Kagoshima City, Kagoshima 890-8520, Japan; thiroshi@m3.kufm.kagoshima-u.ac.jp

Received 28 December 2012
Accepted 11 March 2013

ABSTRACT

Background and aims In mitochondrial myopathy, autophagy is presumed to play an important role in mitochondrial dysfunction. Rimmed vacuoles (RVs), a sign of autophagy, can be seen as a secondary phenomenon in muscle ragged-red fibres (RRFs), whereas the uncommon presentation is that some fibres contain RVs, but without any mitochondrial abnormalities. To investigate the pathogenesis beneath this pathological phenomenon.

Methods We reviewed 783 skeletal muscle specimens and selected five obtained from patients with suspected mitochondrial myopathy, characterised by clearly visible autophagic vacuoles in non-RRFs, besides the coexistence of RRFs and cytochrome oxidase-negative fibres. Immunohistochemical staining with LC-3, and electron microscopy studies were performed. Using resequencing microarray and a next-generation sequencing system, the mitochondrial DNA was screened for mutations and the heteroplasmic level was measured in skeletal muscle and blood.

Results Muscle fibres with RVs and RRFs, as well as some morphologically normal fibres, stained strongly for LC-3. Electron microscopy disclosed significant abnormal mitochondrial proliferation and existence of autophagic vacuoles. After mutation screening, m.8344A>G in the tRNA^{Lys} gene was detected in two patients. The heteroplasmy of mutated G was 45.1% in skeletal muscle and 17.8% in blood in patient 1; patient 2 exhibited 80.3% mutated G in skeletal muscle and 25.2% in blood.

Conclusions These findings demonstrate a new pathological phenotype for the m.8344A>G mutation-related disease and also provide pathological evidence of a correlation between mitochondrial abnormalities and autophagy.

INTRODUCTION

Autophagy generally has a cytoprotective function, often preceding cellular apoptosis or necrosis. Cellular vacuoles that contain fragments of cell components are called autophagic vacuoles. Rimmed vacuoles (RVs) are characterised by small vacuoles lined by many red granules (the 'rim'), as observed by modified Gomori trichrome (mGT) staining and contain fragments of cellular components, including membrane whorls, as observed under electron microscopy. The RVs represent a type of autophagic vacuole and are non-disease-specific structures found in various myopathies, particularly in hereditary inclusion body myopathy, distal myopathy with RVs and inclusion body myositis (IBM).¹ Autophagy also contributes to the degradation of mitochondria (mitophagy),² and

dysfunctional mitochondria may trigger the activation of the autophagic pathway.³

Ragged-red fibres (RRF) are characterised by the existence of subsarcolemmal zones of bright red or reddish blue material in mGT stain (figure 1), which result from the accumulation of abnormal mitochondria beneath the sarcolemma of muscle fibres. Histochemical demonstration of RRFs and cytochrome c oxidase-negative fibres on muscle biopsy is considered to be the hallmark of a mitochondrial myopathy.⁴ In our experience, RVs can be seen in the RRFs, as a secondary change of abnormal mitochondrial accumulation. On the other hand, it has been shown that frequent RRFs can be found in patients with IBM and may reflect an age-related decline in muscle mitochondrial oxidative metabolism.⁵ Nevertheless, in five Japanese patients with suspected mitochondrial myopathy, we found that besides the prominent feature of RRFs, noticeable RVs appeared in the non-RRFs—an unexpected phenomenon.

m.8344A>G mutation in the tRNA^{Lys} gene can result in a myoclonic epilepsy with RRF (MERRF syndrome) and is present in over 80% of affected subjects. Genetic analysis showed an m.8344A>G mutation in two of our patients. Typical MERRF syndrome is characterised by myoclonic epilepsy, cerebellar ataxia and RRFs in skeletal muscle tissue.⁶ However, in this study, the phenotypes of the two patients with the m.8344A>G mutation were atypical; they had proximal muscle weakness and external ophthalmoplegia or preferential facioscapulothoracic muscle involvement.

We demonstrate a new pathological phenotype for the m.8344A>G mutation. These findings suggest a distinct pathogenesis between mitochondrial abnormalities and autophagy. The isolated autophagic vacuoles may also be associated with the atypical clinical phenotype of patients with an m.8344A>G mutation.

MATERIALS AND METHODS

Subjects

We examined 783 skeletal muscle specimens obtained from patients who were referred to our department between 2001 and 2011. Twenty-seven patients with definite coexistence of RRFs and RVs were selected, and then those with IBM (10 patients), dermatomyositis (three patients), polymyositis (one patient), amyotrophic lateral sclerosis (two patients), myotonic dystrophy (one patient) and non-specific myopathy (five patients) were excluded. Based on the clinical features, marked RRFs and cytochrome c oxidase-negative fibres in pathology, five Japanese patients with suspected

To cite: Yuan J-H, Sakiyama Y, Higuchi I, et al. *J Clin Pathol* Published Online First: [please include Day Month Year] doi:10.1136/jclinpath-2012-201431

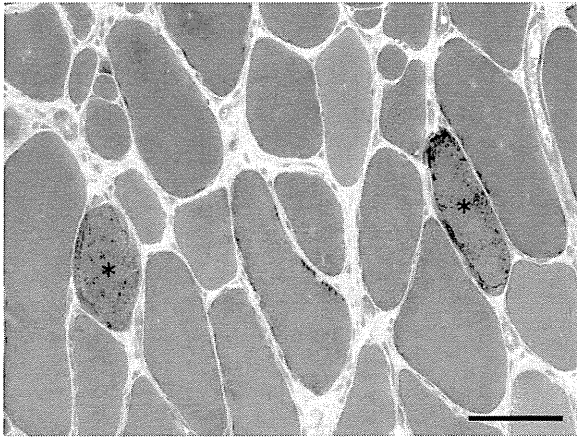


Figure 1 Modified Gomori trichrome staining of muscle ragged-red fibres (RRFs). RRFs are indicated by (*). Bar=100 μ m.

mitochondrial myopathy were chosen for this study. Of these patients, only two who had the m.8344A>G mutation are described herein. No pathogenic mutation was detected in mtDNA from the other three patients. In addition, between 2001 and 2011, we identified the m.8344A>G mutation in blood from six of 169 patients with suspected mitochondrial disorders. Three of these patients underwent a muscle biopsy: two patients comprised the patients previously selected and the other exhibited a typical MERRF syndrome. However, because no definite RVs were seen in skeletal muscle, this last patient was excluded from the study.

All the diagnoses were made by experienced neurologists and pathologists based on clinical and laboratory examinations, electrophysiological studies and skeletal muscle pathology.

Patient 1

A 51-year-old man with no family history of myopathy complained of general fatigue which he had had for 15 years. He began to experience muscle weakness from 36 years of age. This weakness gradually worsened, and by the age of 40 years he had difficulty in walking. Over the following 3 years, the symptoms progressed until he was incapable of lifting any substantial weight. Physical examination showed moderate muscle weakness in the facial, cervical and proximal muscles. His eye movements were also restricted in the superoinferior direction and he had difficulty hearing high-pitched voices. His serum creatine kinase level was raised at 1378 U/l (normal range 45–163 U/l).

Patient 2

A 54-year-old man reported a 24-year history of muscle weakness; there was no family history of any such difficulty. At 30 years of age, he experienced difficulty in lifting his arms and his cervical muscles gradually became affected. He occasionally tumbled down staircases; one fall required admission to hospital for a subarachnoid haemorrhage. Physical examination at the time of study enrolment showed marked weakness and wasting of the shoulder girdle muscles, without scapular winging. The facial muscles, intrinsic muscles of the hand and thigh muscles were also found to be atrophied. The extraocular muscles and the cranial nerves were normal and no other abnormalities were detected. His serum creatine kinase level was 46 U/l. CT indicated myoatrophy in his arms.

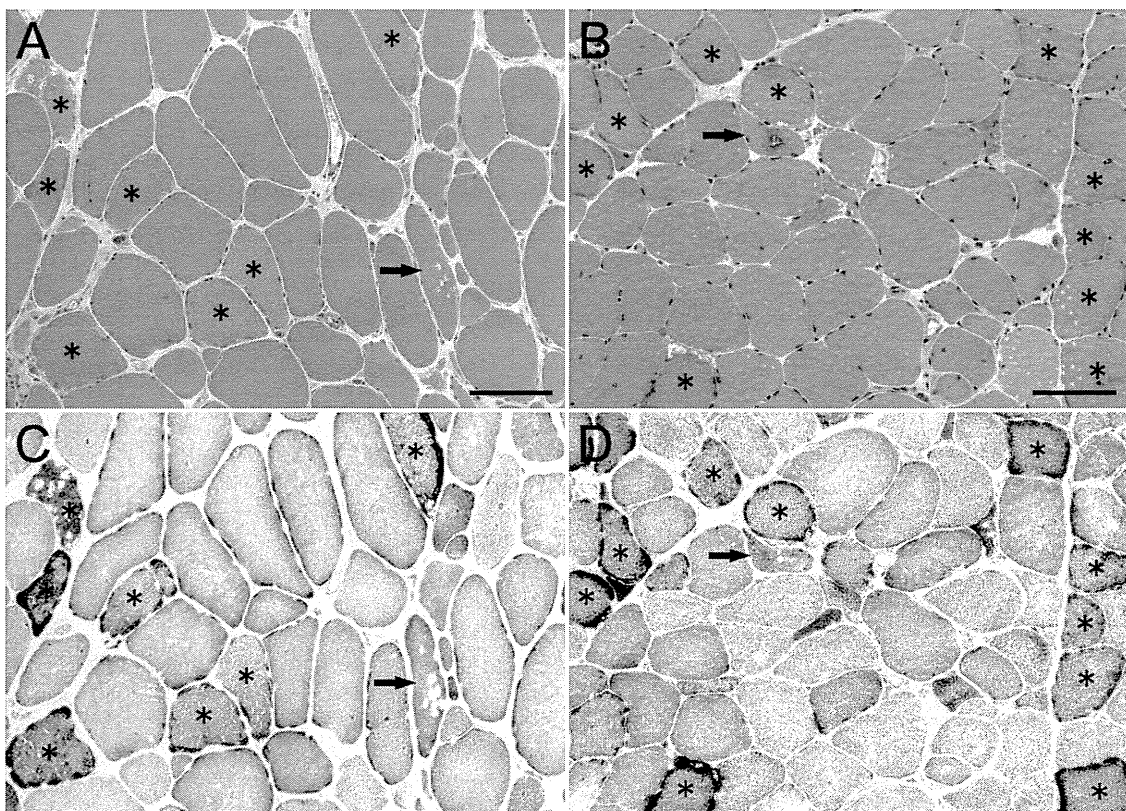


Figure 2 Histochemical staining of muscle ragged-red fibres (RRFs) and isolated rimmed vacuoles in patient 1 (A and C) and patient 2 (B and D). Haematoxylin and eosin (A and B) and succinate dehydrogenase (C and D) staining shows numerous RRFs (*), coexisting with non-RRFs containing rimmed vacuoles (arrow). Bar=100 μ m.

We carried out a neurological examination and neuroradiological study in both patients and no comorbidities, including vascular disease, were seen, except for traumatic subarachnoid haemorrhage in patient 2.

Pathological studies

Skeletal muscle samples were obtained from the biceps brachii. Serial frozen sections (8 µm) were prepared and stained with multiple histochemical methods (see online supplementary table 1).

Other sections prepared on aminosilane-coated slides were immunohistochemically stained with 1:50 diluted microtubule-associated protein 1 light chain 3B (LC-3) clone 5F10 (Nano Tools, France). Biotinylated anti-mouse IgG was used as the secondary antibody and the avidin-biotin-peroxidase complex (ABC) method was used for signal detection (ABC kit; Vector Laboratories, Burlingame, California, USA). All the immunohistochemical procedures were performed as reported previously.⁷

A small amount of the muscle specimens was fixed in glutaraldehyde in cacodylate buffer, post-fixed in 1% buffered osmium tetroxide and then embedded in Epon. Semi-thin sections were prepared for light microscopy to localise the target region, while ultra-thin sections were cut and stained with uranyl acetate and lead citrate for electron microscopy. The electron microscopy procedures were performed as described previously.⁸

Mitochondrial DNA analysis

Genome DNA was extracted from both peripheral blood leucocytes (Qiagen, Maryland, USA) and frozen muscle specimens using a DNeasy blood and tissue kit (Qiagen). The entire mitochondrial DNA extracted from the skeletal muscles was sequenced using MitoChip V2.0 (GeneChip Human Mitochondrial Resequencing Array 2.0) and analysed on GeneChip Sequence Analysis Software V4.0.⁹⁻¹⁰ Previously described primers were used,¹¹ and the variations detected by MitoChip V2.0 were then confirmed by direct Sanger sequencing, as described.¹²

The polymorphic and pathogenic natures of the confirmed mutations were checked against two databases: MITOMAP (<http://www.mitomap.org/>) and GiiB-JST mtSNP (<http://mtsnp.tmig.or.jp/mtsnp/index.shtml>).

Heteroplasmic study

The GS Junior platform can sequence 1 00 000 single PCR fragments in parallel, which enables the detection of low levels of mtDNA heteroplasmy.¹³⁻¹⁴ Using the Primer 3 program, we designed oligonucleotide primers flanking the m.8344A>G mutation (forward: 5'-CACTTTCACCGCTACACGAC-3' and reverse: 5'-GCAATGAATGAAGCGAACAG-3'), which will generate a 428 bp PCR product. Using 50 ng genomic DNA from both blood and skeletal muscle of the two patients, after hot-start PCR, the products were sequenced on the GS Junior platform (Roche-454 Life Sciences, Basel, Switzerland) in accordance with the manufacturer's protocol. The results were assembled using the reference sequence (NC_012920) and analysed using GS Reference Mapper (454 Life Science) software.¹⁵

RESULTS

Pathological studies

In patients, histopathology showed moderate variation in muscle fibre size; numerous degenerating fibres with occasional regenerating or necrotic fibres were seen. RRFs were detected in 12.4% of muscle fibres (497/4001) in patient 1 and 20.7% of muscle fibres (253/1220) in patient 2. RVs were seen in occasional non-RRFs (figure 2). Cytochrome c oxidase activity

was significantly decreased or absent in many fibres, particularly the RRFs, in which high succinate dehydrogenase expression was observed. The cytochrome c oxidase activity was increased in the non-RRF fibres containing isolated RVs. No blood vessels were seen that showed strong succinate dehydrogenase reactivity. Muscle fibres with RVs and RRFs, as well as some morphologically normal fibres, stained strongly for LC-3 (figure 3).

Electron microscopy in the biopsied muscle of the two patients disclosed significant abnormal mitochondrial proliferation with paracrystalline inclusions and circular arrangements of cristae. Autophagic vacuoles with membranous whorls and myelin-like structures were also seen (figure 4).

Mitochondrial DNA analysis

Using MitoChip V2.0, 57 mitochondrial DNA variations were detected in skeletal muscle samples from the two patients and 54 were confirmed to be single nucleotide polymorphisms (SNPs) by referring to the MITOMAP and GiiB-JST mtSNP databases. An m.8344A>G mutation in the tRNA^{Lys} gene was detected in both patients and subsequently confirmed by direct sequencing of DNA from both muscle and blood lymphocytes (figure 5). In addition, a new SNP, m.306C>A in the non-coding area and a missense mutation m.3433T>A (Tyr43Asp) in the ND1 gene of patient 2 were also found. However, considering the vital role of the tRNA^{Lys} gene, we considered m.8344A>G to be the causative mutation.

Heteroplasmic study

Using the GS Junior platform, we clonally amplified and read more than 100 copies of each original amplicon from blood and muscle, in both patients. The percentage of 8344G in patient 1 was 17.8% (23/129) in blood and 45.1% (142/315) in muscle. In patient 2, the percentage was 25.2% (81/321) in blood and 80.3% (598/745) in muscle (figure 5).

DISCUSSION

We selected five patients with suspected mitochondrial myopathy and characterised by the coexistence of RRFs and isolated RVs in muscle fibres. Using a resequencing microarray and a next-generation sequencing system, we identified both the m.8344A>G mutation and its heteroplasmic nature in two of these patients.

m.8344A>G, with a prevalence rate of no more than 0.25/100 000 in Europe, is the most common mutation of MERRF syndrome.¹⁶⁻¹⁸ The clinical variations of MERRF syndrome are extensively expanded to encephalitis, infantile putaminal necrosis, depression, Parkinson's disease, cardiomyopathy, neuropathy, ophthalmoplegia, chronic pancreatitis and the MELAS phenotype that comprises mitochondrial encephalomyopathy, lactic acidosis and stroke-like episodes.¹⁹⁻²⁶ In our study, patient 1 had progressive proximal muscle weakness, restriction of superior-inferior eye movement and hearing loss. Patient 2 experienced isolated skeletal muscle effects, with involvement of the facial and proximal upper limb muscles. Although they harboured the MERRF mutation, both patients presented with nearly isolated myopathy rather than the typical MERRF syndrome with myoclonus epilepsy or cerebellar ataxia.

RRFs formed the predominant pathological feature in 12.4% and 20.7% of fibres in patients 1 and 2, respectively. The combination of cytochrome c oxidase-negative fibres and abnormally proliferated mitochondria found in electron microscopy, confirmed the pathological diagnosis of mitochondrial myopathy. In both patients haematoxylin and eosin and mGT staining

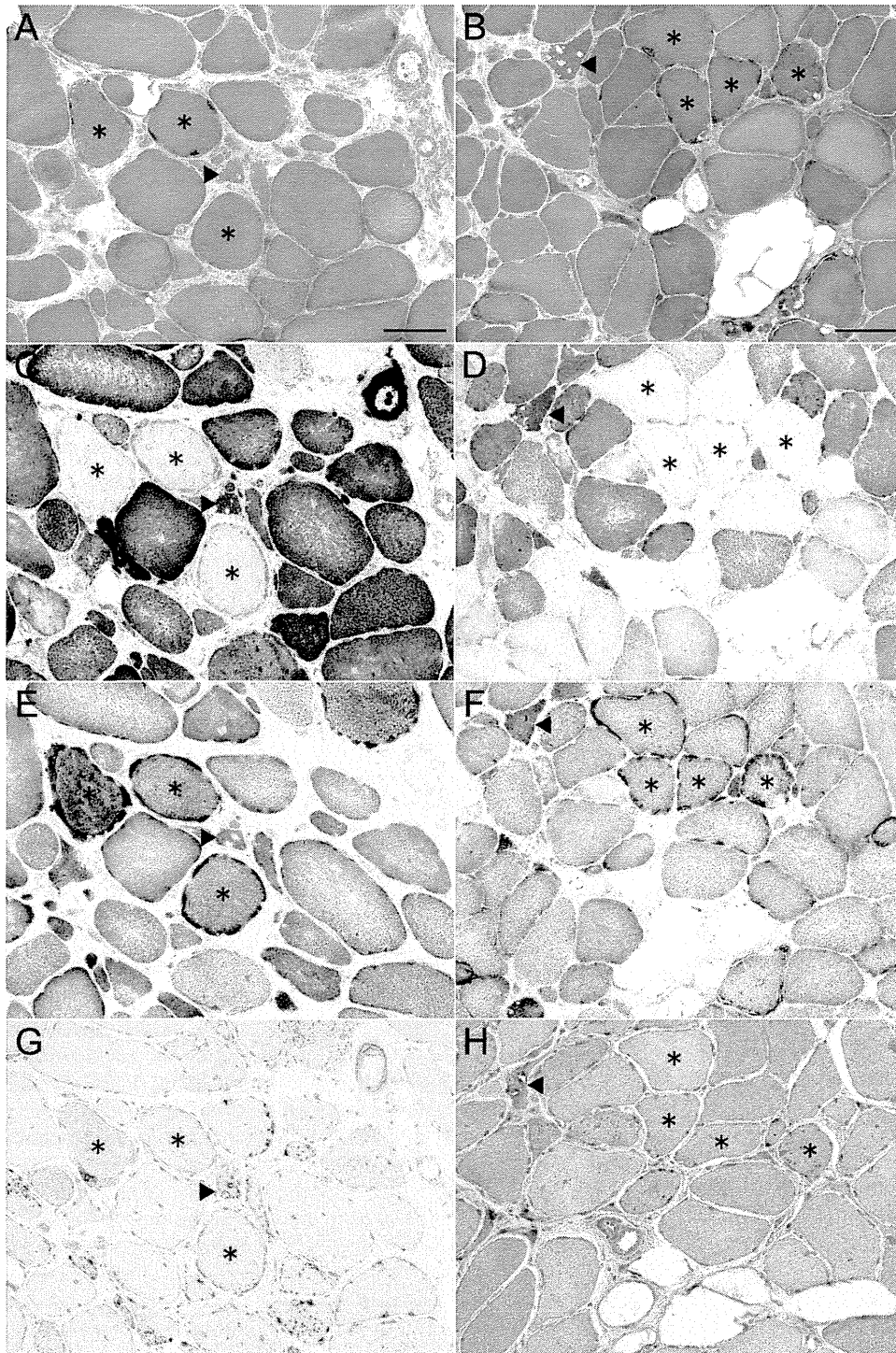


Figure 3 Serial sections of histochemical and immunohistochemical stained skeletal muscle samples in patient 1 (A, C, E and G) and patient 2 (B, D, F and H). Moderate myopathic change with coexistence of numerous in muscle ragged-red fibres (RRFs) (*) and some rimmed vacuoles (▲) is seen with the modified Gomori trichrome stain (A and B). Cytochrome c oxidase activity is significantly decreased or absent in many fibres, particularly RRFs (C and D), with high succinate dehydrogenase expression (E and F). Immunohistochemical staining of LC-3 was strong in fibres with rimmed vacuoles and RRFs and also in some morphologically normal fibres (G and H). Bar=100 μ m.

demonstrated RVs in fibres without mitochondrial accumulation or loss of cytochrome c oxidase activity. LC-3 aggregation was seen in fibres with isolated RVs, RRFs with secondary vacuolation and even in some fibres without any morphological changes. These abnormalities suggest the overexpression of autophagy or disorders of autophagic pathways in these fibres.²⁷ Electron microscopy also confirmed the existence of autophagic

vacuoles. Although mild autophagic changes can be seen in RRFs of patients with common mitochondrial myopathies, conspicuous RVs and LC3-positive fibres in non-RRFs were the characteristic findings in both of our study patients. Additionally, degeneration, regeneration or necrosis of muscle fibres indicated active cellular damage, probably resulting from mitochondrial dysfunction.